STRUCTURAL EFFECT OF THE ZINC ELECTRODE ON ITS DISCHARGE PERFORMANCE

T. S. CHANG, Y. Y. WANG and C. C. WAN

Department of Chemical Engineering, National Tsing Hua University, Hsinchu, Taiwan (Republic of China)

(Received September 18, 1982; in revised form December 17, 1982)

Summary

The formation conditions in the preparation of zinc electrodes for the nickel–zinc battery were varied to obtain different electrode structures. The porosity and pore size distribution of the zinc electrode were found to be dominant factors in determining the electrode capacity. The optimal porosity was estimated to be about 0.64.

Introduction

The nickel–zinc battery has been recognized as one of the main potential power systems to replace the lead–acid battery in the application of electric vehicles. It has a fairly high specific energy and power and it also performs satisfactorily in a low temperature environment. Its major shortcomings, such as shape change, crystal densification and dendrite growth, have been significantly ameliorated in recent years due to intensive research and technological improvements [1 - 10]. Although it is generally recognized that the pore structure of the zinc electrode is essential in controlling the discharge capacity [11 - 14], quantitative analysis in this respect is still insufficient. The objective of this study is to formulate an equation which can correlate, within reasonable accuracy, the relation between pore structure and electrode capacity when the dissolution of the discharge product is considerable, as, for example, with a zinc electrode.

Theoretical

The quantitative prediction of electrode capacity has been investigated by previous workers. Newman and Tobias [15] first proposed a continuous macrohomogeneous model to calculate the electrode capacity and potential. Selanger [16] established a porosity diagram to estimate capacity based on the density change of different materials in the electrode. However, his

0378-7753/83/$3.00

assumption that all the pores would be completely filled by the product could lead to considerable error [17]. Tong *et al.* [17] deduced a semi-empirical formula to estimate the capacity of the iron electrode of the nickel–iron battery. However, their assumptions that the electrode volume remains constant in the discharge process, and the products are insoluble, are invalid in the case of the zinc electrode. Their equation was consequently modified in this study.

For an electrochemical reaction

$$\nu_1 A_1(s) + \nu_2 A_2(aq) \rightleftharpoons \nu_3 A_3(s) + \nu_4 A_4(aq) + ne^- \tag{1}$$

and a subsequent product dissolution process

$$\nu_3 A_3(s) + \nu_2 A_2(aq) \rightleftharpoons \nu_5 A_5(aq) + \nu_6 A_6(aq) \tag{2}$$

we define an experimental parameter, ∂, as the ratio of the dissolution rate of A_3 to its generation rate

$$\partial = \frac{\text{No. of moles of } A_3 \text{ dissolved}}{\text{No. of moles of } A_3 \text{ generated}} \tag{3}$$

If the product is insoluble, *e.g.*, $Fe(OH)_2$ of the Fe electrode, then $\partial = 0$. The number of moles of A_3 after discharge per mole of product is $1 - \partial$ and the volumetric change of the solid phase in the electrode is consequently $[(1 - \partial)\nu_3 V_{A_3} - \nu_1 V_{A_1}]It/nF$ where V_{A_3}, V_{A_1} are the molar volumes of A_3, A_1 and I and t are the discharge current and time, respectively.

Assuming the solid phase contains only active material and the initial porosity ϵ_1 is defined as

$$1 - \epsilon_1 = \frac{1}{V_1}\left(\frac{m_{A_1}}{\rho_{A_1}}\right) \tag{4}$$

then the volume of solid phase after discharge is

$$\frac{m_{A_1}}{\rho_{A_1}} + [(1 - \partial)\nu_3 V_{A_3} - \nu_1 V_{A_1}]\,\frac{It}{nF}$$

Hence

$$1 - \epsilon_2 = \frac{1}{V_2}\left[\frac{m_{A_1}}{\rho_{A_1}} + [(1 - \partial)\nu_3 V_{A_3} - \nu_1 V_{A_1}]\,\frac{It}{nF}\right] \tag{5}$$

where V_1, V_2 are the electrode volumes before and after discharge, m_{A_1} is the initial mass of A_1, ρ_{A_1} the true density of A_1 and ϵ_2 is the porosity after discharge.

Multiplying eqn. (5) on both sides by V_2/V_1, we have

$$\frac{V_2}{V_1}(1 - \epsilon_2) = \frac{1}{V_1}\left[\frac{m_{A_1}}{\rho_{A_1}} + [(1 - \partial)\nu_3 V_{A_3} - \nu_1 V_{A_1}]\,\frac{It}{nF}\right] \tag{6}$$

Substracting eqn. (4) from eqn. (6) and after rearrangement,

$$It = \frac{\epsilon_1 - [1 - (V_2/V_1)(1 - \epsilon_2)]}{1 - \epsilon_1} \frac{nF}{(1 - \partial)\nu_3 V_{A_3} - \nu_1 V_{A_1}} \frac{m_{A_1}}{\rho_{A_1}} \tag{7}$$

The specific capacity C_p which is defined as It/m_{A_1} is

$$C_p = \frac{\epsilon_1 - [1 - (V_2/V_1)(1 - \epsilon_2)]}{1 - \epsilon_1} \frac{1}{(1 - \partial)\nu_3 V_{A_3} - \nu_1 V_{A_1}} \frac{nF}{\rho_{A_1}}$$

$$= \frac{\epsilon_1 - [1 - (V_2/V_1)(1 - \epsilon_2)]}{1 - \epsilon_1} K \tag{8}$$

where

$$K = \frac{1}{(1 - \partial)\nu_3 V_{A_3} - \nu_1 V_{A_1}} \frac{nF}{\rho_{A_1}} \tag{9}$$

When the electrolyte concentration, temperature, and discharge current are kept constant, K becomes a constant and can be experimentally determined.

In our case, eqns. (1) and (2) are

$$Zn(s) + 2(OH)^-(aq) \rightleftharpoons Zn(OH)_2(s) + 2e^- \tag{10}$$

$$Zn(OH)_2(s) + 2(OH)^-(aq) \rightleftharpoons Zn(OH)_4^{2-}(aq) \tag{11}$$

Therefore $\nu_1 = \nu_3 = 1$, $A_1 = Zn$, $A_3 = Zn(OH)_2$ and $n = 2$.

The prediction of maximum specific capacity, C_p, is of engineering significance and can be calculated based on the following conditions:

(1) When the volumetric reduction of reactant is equal to the volumetric increase of product, *i.e.*, $(1 - \partial)\nu_3 V_{A_3} = \nu_1 V_{A_1}$, then the porosity will remain constant and C_p should be equal to its theoretical specific capacity. For the zinc electrode, $\partial = 0.719$.

(2) When $\partial > 0.719$, that is, the volumetric reduction of the reactant is larger than the volumetric increase of the product, the porosity should increase as discharge proceeds. The electrode will not stop discharging as a result of blocking of the electrolyte passages, the C_p should also be equal to its theoretical specific capacity.

(3) When $\partial < 0.719$, the porosity will gradually decrease and the discharge process will stop when all the electrolyte passages are blocked. The capacity is controlled by eqn. (8).

In reality, the electrolyte is virtually completely blocked when the porosity is reduced to 0.1. Therefore, if we set the final porosity ϵ_2 at 0.1, eqn. (8) becomes

$$C_p = \frac{\epsilon_1 - [1 - 0.9(V_2/V_1)]}{1 - \epsilon_1} K \tag{12}$$

where

$$K = \frac{1}{(1 - \partial)V_{Zn(OH)_2} - V_{Zn}} \frac{2F}{\rho_{Zn}} \tag{13}$$

Assuming $V_2 = V_1$, eqn. (12) can be simplified to

$$C_p = \frac{\epsilon_1 - 0.1}{1 - \epsilon_1} K \tag{14}$$

If we further assume that the product is insoluble, *i.e.*, $\partial = 0$, then

$$C_p = \frac{\epsilon_1 - 0.1}{1 - \epsilon_1} K' \tag{15}$$

where

$$K' = \frac{1}{V_{Zn(OH)_2} - V_{Zn}} \frac{2F}{\rho_{Zn}} = 0.3205$$

and becomes a constant. Equation (15) is identical with Tong's model [17] and K' is 0.7076 for an iron electrode.

If we set $\epsilon_2 = 0$, which implies that the discharge should stop when all the pores are blocked, then eqn. (15) is changed to

$$C_p = \frac{\epsilon_1}{1 - \epsilon_1} K' \tag{16}$$

which is identical with Selanger's model [16].

Experimental

Preparation of zinc electrodes

1.6 g of active material mixture (97% ZnO, 3% HgO) was mixed with 0.6 g of 6% polyvinyl alcohol solution. The paste was applied to a stainless steel (60 mesh) screen and dried at 30 °C for 40 min. The plate was then pressed at 60 kg/cm^2 to flatten it and to compress the reactant particles.

The plate was wrapped with nonwoven fabric and was electroformed in 5% KOH solution at various charging currents and times. The counter electrode was a stainless steel panel. After formation, the plate was rinsed with distilled water.

The electrode was wrapped with nonwoven fabric (FT-218) and a separator (Permion P2190) and was then ready for the discharge test. Two nickel electrodes were used as the counter electrode. The capacity of the nickel electrodes was far in excess of that of the zinc electrode to make the zinc electrode the capacity controlling electrode. 30% KOH solution containing 20 g/l of LiOH was used as the electrolyte. All the chemicals were of reagent grade. The electrode was discharged at 0.15 A until the output voltage dropped to 0.9 V.

The purpose of the experiment was to investigate the effect of formation conditions on the discharge performance and the structure of the electrode.

The mercury penetration method, taking appropriate precautions, was used to measure the pore size distribution of the electrode.

The porosity was calculated according to the following formula

$$\epsilon = \frac{\text{pore volume}}{(\text{true density of active material})^{-1} + \text{pore volume}} \quad (17)$$

and in our case

$$\text{true density of the active material} = 0.97\ \rho_{Zn} + 0.03\ \rho_{HgO} \quad (18)$$

The surface area was measured by the BET method with nitrogen as the adsorption gas.

Results and discussion

Effect of formation conditions

The zinc electrodes were classified as A, B, C, three groups based on different formation currents. As shown in Table 1, each group was subdivided into four according to the ratio of the formation electric quantity to the theoretical electric quantity based on Faraday's law.

Table 2 lists the structural parameters of the various electrodes and Figs. 1, 2 and 3 show their pore size distributions. It is apparent that the formation conditions have a significant effect on the structure of the electrode.

At low formation currents, *i.e.*, the A group of electrodes, increased formation electric quantity tends to reduce the porosity and plate thickness and to increase the small pore fraction. It seems that over-formation causes aggregation of zinc particles. At high formation currents, *i.e.*, the C group,

TABLE 1

Designation of zinc electrodes prepared by various forming conditions

Notation	Forming current (mA)	Forming E.Q./Theor. E.Q.
A-1	300	7
A-2	300	8
A-3	300	9
A-4	300	10
B-1	500	7
B-2	500	8
B-3	500	9
B-4	500	10
C-1	700	7
C-2	700	8
C-3	700	9
C-4	700	10

E.Q. = electric quantity.

TABLE 2

Physical properties of various zinc electrodes

Notation	S	V_p	ϵ_1	P	h	V_2/V_1
A-1	2.7	0.25	0.641	2.564	0.540	0.705
A-2	2.8	0.24	0.632	2.631	0.526	0.732
A-3	2.6	0.22	0.611	2.777	0.499	0.769
A-4	4.5	0.17	0.548	3.225	0.429	0.886
B-1	5.1	0.33	0.702	2.127	0.651	0.573
B-2	2.0	0.28	0.667	2.381	0.580	0.638
B-3	2.8	0.28	0.668	2.381	0.590	0.652
B-4	1.9	0.31	0.689	2.222	0.623	0.634
C-1	6.2	0.25	0.641	2.564	0.540	0.711
C-2	4.0	0.26	0.650	2.450	0.554	0.680
C-3	3.3	0.33	0.702	2.127	0.651	0.574
C-4	5.4	0.28	0.667	2.381	0.580	0.642

S, Surface area (m^2/g); V_p, pore volume (cm^3/g); P, apparent density (g/cm^3); h, thickness (mm); ϵ_1, porosity; V_1, electrode volume before discharge; V_2, electrode volume after discharge.

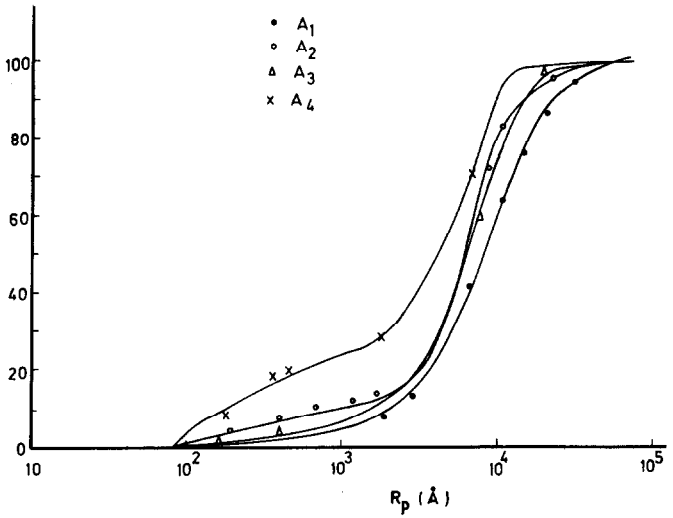

Fig. 1. Pore size distribution of group A.

the surface area is, in general, larger than that of the A and B groups. It is interesting to note that surface area and porosity often vary in opposite directions, which means that the pore size distribution may also be an important factor in determining surface area.

The structural changes due to variation in the formation conditions, in turn, affect the discharge performance. The performances of the electrodes are summarized in Table 3. Since we are mainly interested in the structural effect on the discharge performance, we attempted to find the

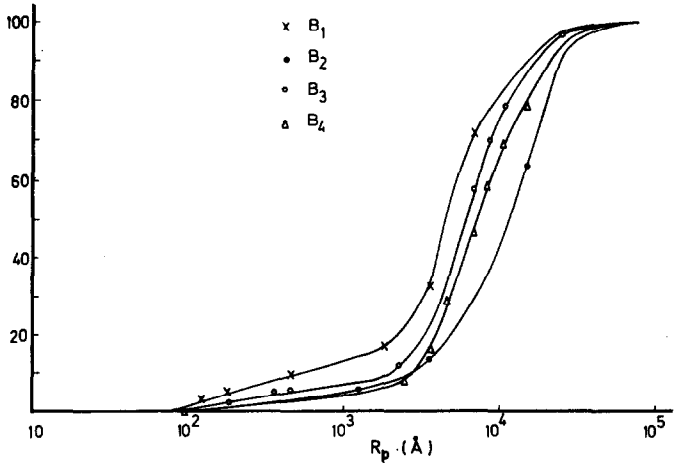

Fig. 2. Pore size distribution of group B.

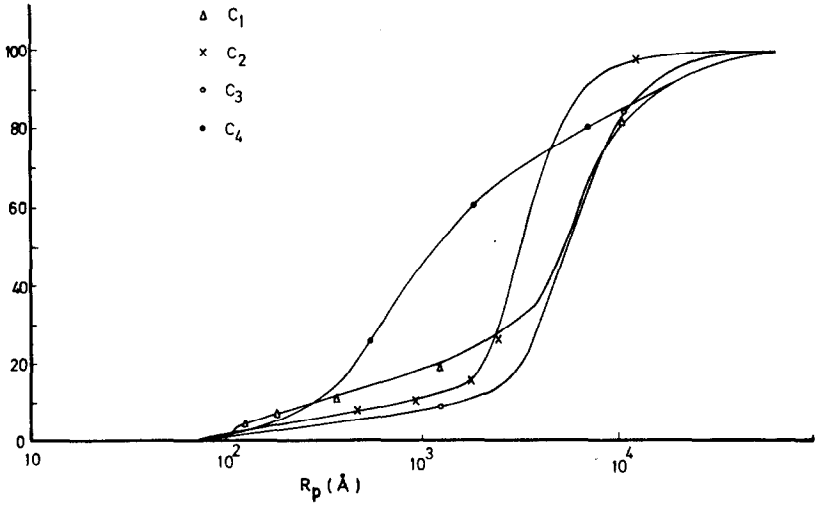

Fig. 3. Pore size distribution of group C.

relation between porosity and specific capacity, which is shown in Fig. 4. If we use specific capacity as the single criterion, the results indicate an optimum porosity around 0.64. When porosity is markedly lower than 0.64, the transport of OH^- ions is inhibited. However, when the porosity is well above 0.64, the structure is very loose and exhibits high electrical resistance which becomes the predominant factor. This is consistent with previous workers' findings [17, 18].

The K value of eqn. (12) depends on the electrolyte concentration and temperature. Increased concentration or temperature favors the dissolution of $Zn(OH)_2$, which implies larger ∂ and K values.

TABLE 3

The capacity density, utilization, and energy density of zinc electrodes prepared by different forming conditions

Notation	Specific capacity (A h/g)	Reactant utilization (%)	Specific energy (W h/g)
A-1	0.545	64.49	0.803
A-2	0.557	65.92	0.855
A-3	0.550	65.01	0.842
A-4	0.545	64.41	0.794
B-1	0.520	61.53	0.786
B-2	0.513	60.70	0.781
B-3	0.541	64.02	0.794
B-4	0.501	59.29	0.770
C-1	0.553	65.44	0.853
C-2	0.533	63.07	0.790
C-3	0.520	61.57	0.783
C-4	0.512	60.51	0.780

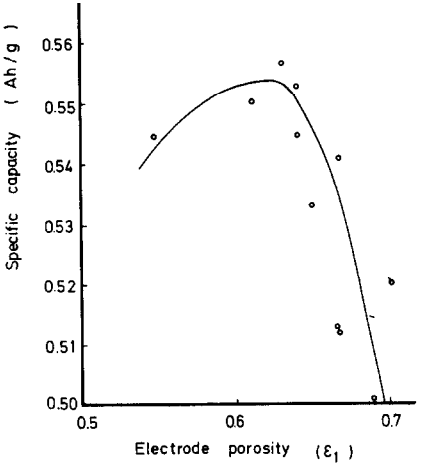

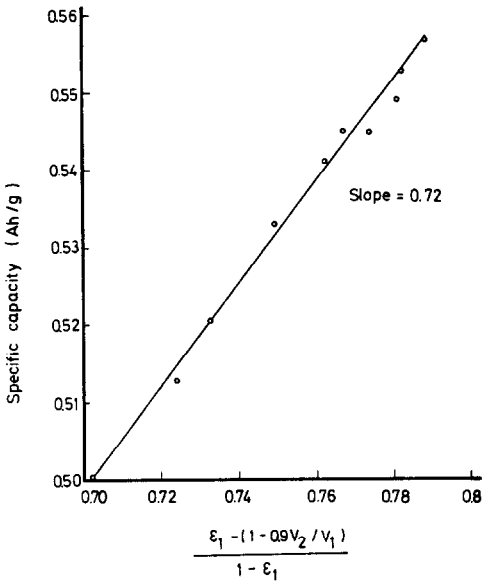

Fig. 4. Relationship between discharge capacity and porosity.

Fig. 5. Specific capacity of zinc electrode *vs.* $\{\epsilon_1 - [1 - 0.9(V_2/V_1)]\}/(1 - \epsilon_1)$.

Figure 5 is a plot of specific capacity *versus* $\{\epsilon_1 - [1 - 0.9(V_2/V_1)]\}/(1 - \epsilon_1)$. The result tends to be a straight line and its slope is the K value. Using the least squares method, the K value was calculated to be 0.72. When K = 0.72, the ∂ value of the zinc electrode is 0.4 according to eqn. (13). This means that during discharge, 0.4 mole of $Zn(OH)_2$ is dissolved

for one mole of $Zn(OH)_2$ generated electrochemically. Only 0.6 mole of $Zn(OH)_2$ remains in the electrode. We mentioned earlier that when $\partial <$ 0.719, the porosity should decrease as discharge continues. The passage of electrolyte is finally blocked and the discharge stops. Consequently, in this case, the porosity determines the specific capacity. The experimentally determined K value takes into account the volume change and dissolution process during discharge. These two factors cannot be neglected in the analysis of the zinc electrode. Their importance is clearly illustrated in Fig. 6.

Figure 6 shows the correlation of specific capacity with porosity as predicted by various models. It is obvious that eqn. (12) best predicts the maximum specific capacity and serves as a quantitative relationship between the electrode structure and the discharge performance for the zinc electrode.

Models developed by Tong [17] and Selanger [16] both neglect the volume change and zinc dissolution effect. Although their predictions are definitely less accurate than that of eqn. (12), they seem better than the prediction according to eqn. (14), which assumes that $V_2 = V_1$ and still takes the dissolution process into consideration. This is because these two

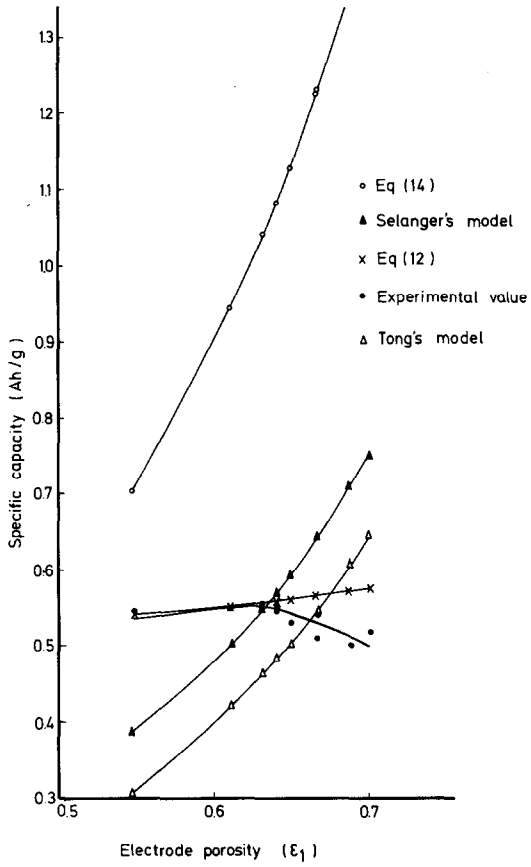

Fig. 6. Specific capacity of zinc electrode *vs.* electrode porosity (ϵ_1).

factors tend to cancel each other. Increased volume change causes reduced capacity but the dissolution of the $Zn(OH)_2$ product facilitates the discharge reaction.

A closer look at eqns. (12), (15) and (16) would lead to a general equation governing the relation between electrode porosity and discharge capacity

$$C_p = \frac{a + b\epsilon_1}{1 - \epsilon_1} K \tag{19}$$

For Selanger's model, $a = 0$, $b = 1$ and for Tong's model $a = -0.1$, $b = 1$. In eqn. (12), $a = 0.75$, $b = -0.665$ in our case. For any specific electrode, a, b and K are its characteristic parameters which can be used to predict its discharge capacity.

Conclusions

1. The volume change and dissolution process are very significant in the discharge of the zinc electrode. Mathematical modelling of this system must take these two factors into account.

A model was developed

$$C_{p\,max} = \frac{\epsilon_1 - [1 - 0.9(V_2/V_1)]}{1 - \epsilon_1} K$$

which can estimate the maximum specific capacity if we assume that the terminal porosity is around 0.1.

2. The zinc electrode is mainly controlled by its porosity which facilitates the transport of reactant and product. An optimal porosity is around 0.64.

List of symbols

A_i ith chemical species
C_p Specific capacity of electrode
F Faraday's constant
I Discharge current
K Characteristic constant
m_{A_i} Mass of A_i before discharge
n Number of electrons transferred in the reaction
t Discharge duration
V_{A_i} Molar volume of A_i
V_1 Electrode volume before discharge
V_2 Electrode volume after discharge
∂ Ratio of A_3 dissolution rate to its generation rate
ϵ_1 Electrode porosity before discharge

ϵ_2 Electrode porosity after discharge
ρ_{A_i} True density of A_i
ν Stoichiometric coefficient

References

1 S. Falk and A. Salkind, *Alkaline Storage Batteries*, Wiley, New York, 1969.
2 C. Wales and A. Simon, *J. Electrochem. Soc., 115* (1968) 1228.
3 J. Bockris, A. Nagy and D. Drazic, *J. Electrochem. Soc., 119* (1972) 285.
4 R. Falsdale, N. Hampson, P. Jones and A. Strachan, *J. Electrochem. Soc., 118* (1971) 213.
5 R. Powers and N. Breiter, *J. Electrochem. Soc., 116* (1969) 719.
6 R. Powers, *J. Electrochem. Soc., 118* (1971) 685.
7 A. Marshall and N. Hampson, *J. Appl. Electrochem., 7* (1977) 271.
8 M. Ciu, G. Cook and N. Yao, *J. Electrochem. Soc., 128* (1981) 1663.
9 L. Gaines, *J. Electrochem. Soc., 116* (1969) 62.
10 Y. Yamazaki and N. Yao, *J. Electrochem. Soc., 128* (1981) 1655.
11 K. Micka, T. Rousar and J. Jindra, *Electrochim. Acta, 23* (1978) 1031.
12 J. McBreen, *J. Electrochem. Soc., 119* (1972) 1620.
13 K. Choi, D. Bennion and J. Newman, *J. Electrochem. Soc., 123* (1976) 1616.
14 S. P. Poa and S. J. Lee, *J. Appl. Electrochem., 9* (1979) 307.
15 J. Newman and C. Tobias, *J. Electrochem. Soc., 109* (1962) 1183.
16 P. Selanger, *J. Appl. Electrochem., 4* (1974) 263.
17 C. Tong, S. Wang, Y. Wang and C. Wan, *J. Electrochem. Soc., 129* (1982) 1173.
18 W. Bryant, *J. Electrochem. Soc., 126* (1979) 1899.